Applications of ICFD /SPH Solvers by LS-DYNA® to Solve Water Splashing Impact to Automobile Body

George Wang (1*), Kevin Gardner (3), Eric DeHoff (1), Facundo del Pin (2), Inaki Caldichoury (2), Edouard Yreux (2)

(1) Vehicle Structure – Automotive Safety
Honda R&D Americas, Inc., 21001 State Route 739, Raymond, OH 43067-9705
(2) Livermore Software Technology Corporation, 7374 Las Positas Road, Livermore, CA, 94551
(3) The Ohio State University, Columbus, OH

*Corresponding author: gwang@oh.hra.com

Key words: fluid-structure interaction, ICFD, SPH, water splashing impact

Abstract

When a vehicle runs at high speed on a watery or muddy road, the high speed splashing generated by tire rotation often causes damage to the underbody panels. This is a challenging dynamic FSI (fluid-structure interaction) problem for Honda to consider. ICFD and SPH are two powerful solutions used in FSI applications, especially for high-speed flow and with dynamic free surface evolution. This paper presents some FSI solutions of water splashing on automotive components by using ICFD and SPH solvers in LS-DYNA®:

(1) Aluminum underbody panel water impact. The panel is impacted by a water balloon shot out of a water cannon that simulates a large water splash contacting the panel. Results with ICFD and SPH solvers are discussed and compared to the corresponding test data from the Ohio State University in Columbus, OH, USA. In brief, the ICFD results of peak displacement/force on the panel caused by the impact agree well with the tests while the SPH method over predicts the load and displacement.

(2) Water splash impact on vehicle. In this study, a model of a half MUV runs at 45 mph into a 0.24 m high water layer. The vehicle bottom surface is set up as a deformable structure while the other parts are rigid. It is shown that the SPH method can easily simulate the realistic water splashing caused by the moving tires and vehicle body, whereas the ICFD solution has a difficult time converging to a solution and also takes much longer to solve.

Introduction

When a vehicle runs at high speed on a watery or muddy road as shown in Fig. 1, the high speed splashing generated by the rotating tires has high energy and often causes damage to the underbody panels. This is a challenging dynamic FSI (fluid-structure interaction) problem for Honda to consider at an early design stage.

Fig. 1 Vehicle under a highly water splashing condition

Recent dramatic developments in computer technology and engineering software make it possible to solve these water splashing problems in modern automobile fields.

FSI in meaning is a coupling process between flow and solid in time and it occurs whenever the flow effect on the structure causes it to deform or even fail. Once the structure is deformed the flow field changes and needs to be updated. To precisely predict these interactions, complicated software is required to simulate both the fluid part and the structural part that evolves over time as the fluid and the structure change during the analysis.

ICFD and SPH of LS-DYNA® are two of the possible solutions used in FSI applications, especially for high-speed flow and with dynamic free surface evolution. In this paper we applied these two methods to our problems to evaluate their accuracy and efficiency.

LS-DYNA® Version R8.1 [1] double precision includes the incompressible flow solver (ICFD) which uses the implicit solver to solve the strong FSI process listed in Fig. 2 [2]. The LS-DYNA ICFD solver has been applied to many FSI applications and good results have been shown [3-7].

SPH is included in LS-DYNA® [8]. It is a Lagrangian method for solving partial differential equations with the domain discretized by a series of roughly equal-spaced particles. Since it was first proposed in 1977 [9], SPH has been continually improved and is more and more widely used in various industrial fields as a reliable and robust solver [10-12]. An SPH work process is shown in Fig. 3.

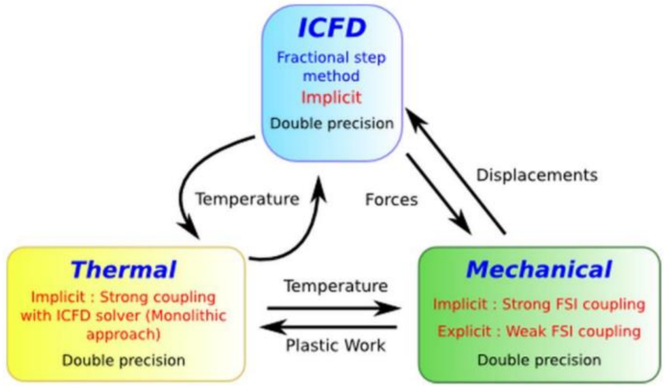

Fig. 2 FSI solver process in LS-DYNA®ICFD [2]

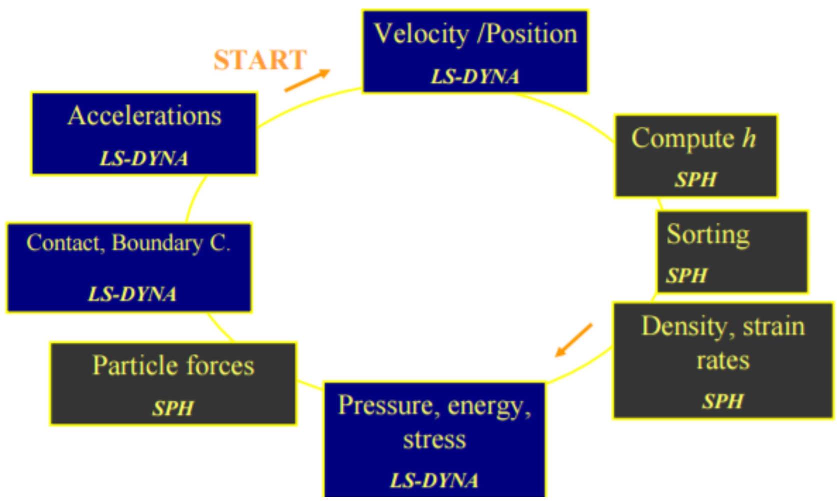

Fig. 3 SPH work process in LS-DYNA® [8]

In this paper, two FSI solutions to water impact to automobile body are presented:

(1) First, we solve aluminum underbody panel impacted by a water balloon shot out of a water cannon. Results with ICFD and SPH solvers are discussed and compared with the corresponding test data (displacement and force) from the Ohio State University in Columbus, OH, USA.

(2) Second, we develop a half-MUV vehicle FSI model using ICFD and SPH methods. Water splashing is modeled by the two methods and the efficiency between the two models is revealed.

Results

1. Underbody panel impacted by a water balloon shot out of a water cannon

1.1 Model setup

The tests were conducted at Ohio State University (OSU), Ohio, USA. Fig. 4 (a) and (b) show the water cannon test set up and the CAE model setup according to the tests, respectively. The volume of water inside the balloon is 120 mL; the diameter of the cannon pipe is 3 inch with a standoff of 24 inch to the aluminum panel of 0.8 mm in thickness. The balloon is not considered in the CAE model. The water body is approximated as a circular cylinder with a depth of 26.3 mm to equalize the total water mass in the balloon. The panel is secured at each corner by a steel beam fixture. The measurement of displacement at the center (DIC) and the total axial support force of the four beams is compared with the ICFD/SPH results.

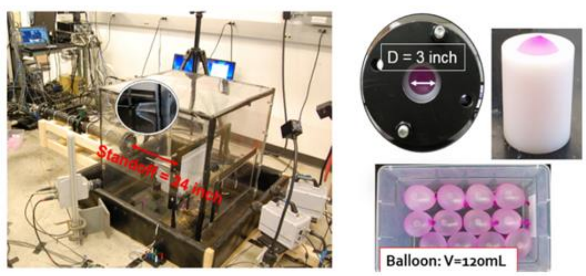

(a) Water cannon test set up

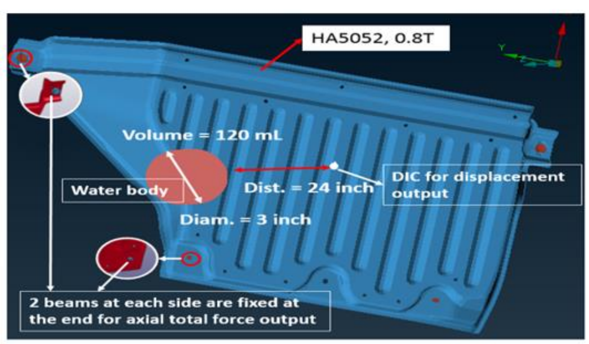

(b) CAE model set up

Fig. 4 Illustration for underbody panel impacted by a water balloon shot out of a water cannon

Three panels were tested. From the high-speed camera video data obtained at OSU, the water velocities right before contact to the panel can be measured and are listed in Table 1.

Table 1 Initial velocity of water body in CAE model

Panel #	Initial velocity (m/s)
2	25.4
3	30.5
4	27.9

Fig. 5 (a-b) shows the assembled ICFD fluid surface mesh and solid structure mesh in the CAE model. Two-way strong coupling is used in FSI process. A circular cylinder (Pid =1) approximates the water body with initial velocities shown in Table 1. A non-slip condition is set at the flow boundary at pid = 2, and the pressure condition is set to lateral boundary (pid = 3). LES is selected for modeling the turbulent flow.

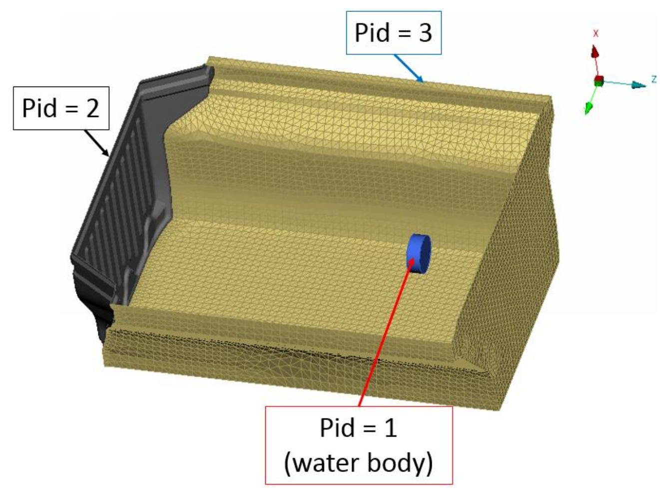

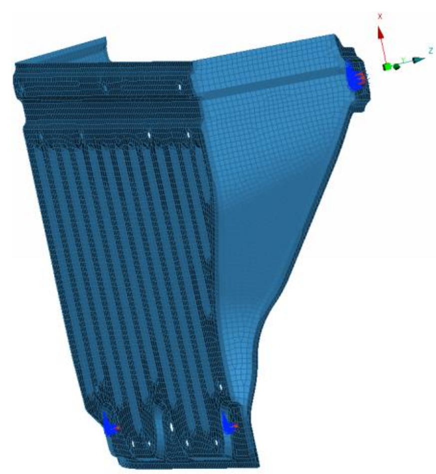

(a) ICFD fluid surface mesh (b) Solid structure mesh

Fig. 5 Assembled CAE mesh for underbody panel impacted by a balloon shot out of cannon

Fig. 6 shows the SPH model. The water body is approximated by SPH particles with *MAT9. The total number of SPH nodes is 72530. The LS-DYNA d3hsp file shows that the total particle mass 0.11999981E-03 T matches the mass of the 120 mL of water in the balloon.

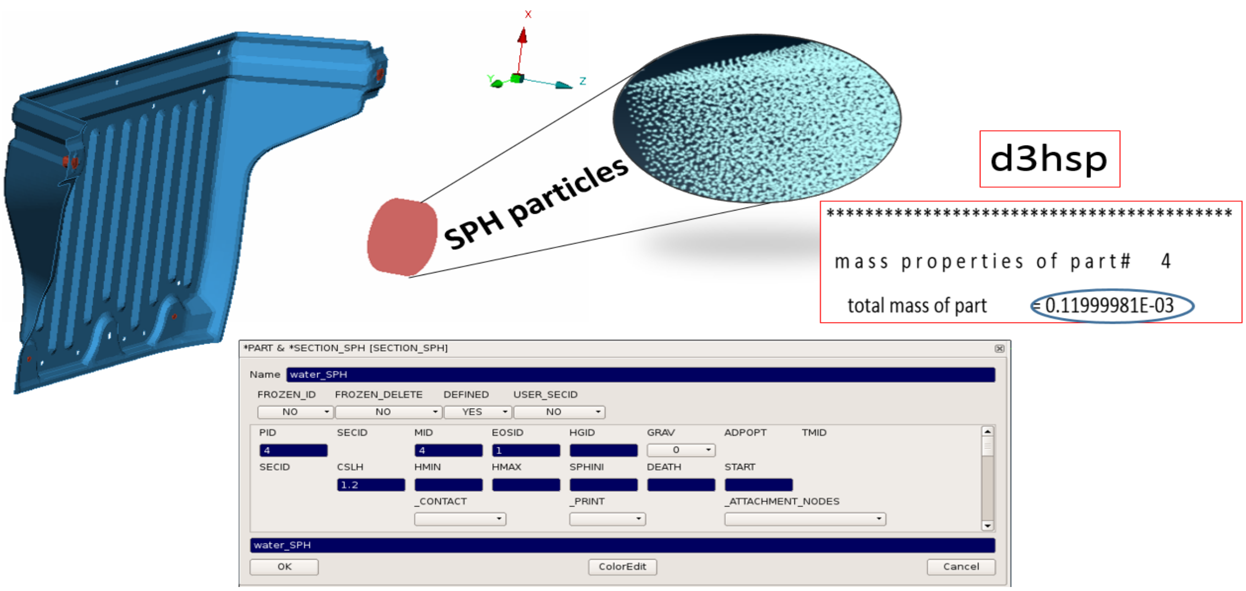

Fig. 6 SPH model for underbody panel impacted by a water balloon shot out of a water cannon.

1.2 ICFD/SPH vs experiments

Fig. 7 shows a comparison of displacement and force profiles predicted by ICFD with the according experiments. Fig. 8 (a, b) shows a snapshot of the permanently deformed panel predicted by ICFD and in the test. It is seen that the ICFD results show good correlation with the experimental data.

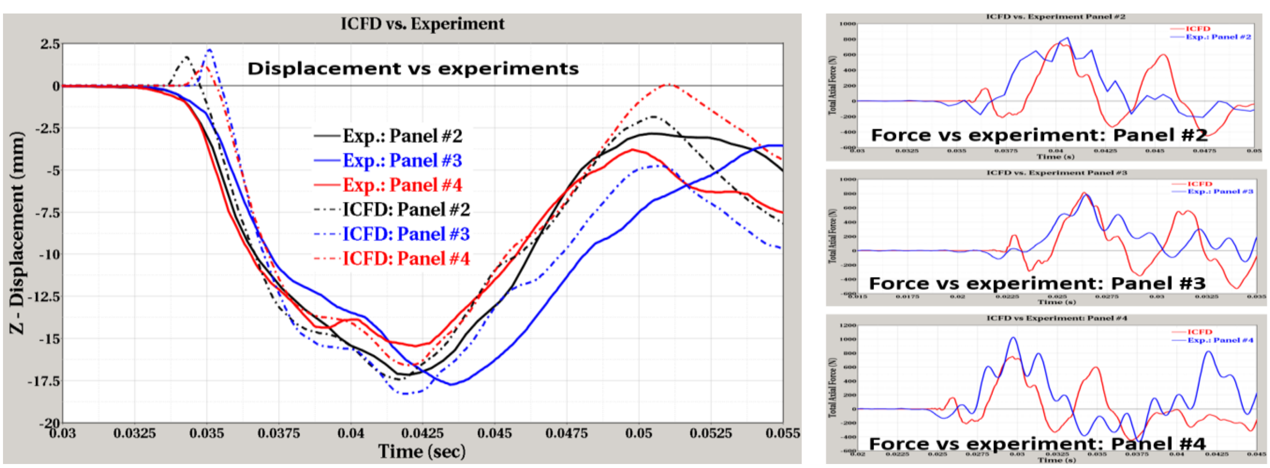

Fig. 7 Comparison of displacement (ICFD – dot lines; experiment – solid lines) and force (ICFD – red lines; experiment – blue lines) profiles by ICFD with experiments.

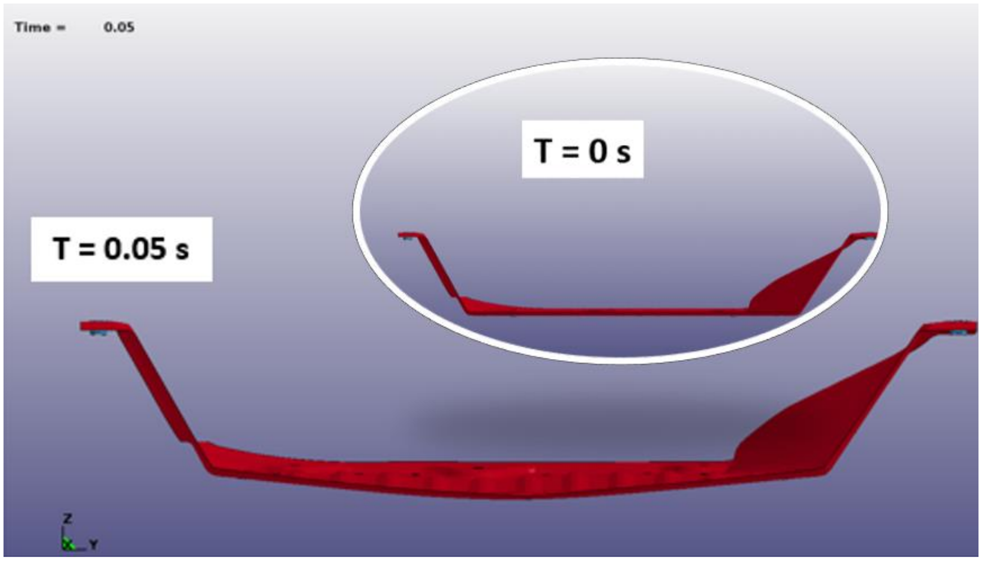

(a) ICFD

(b) Experiment

Fig. 8 Snapshot of permanently deformed panel

Fig. 9 shows a comparison of the profiles of displacement at the center of panels and the total axial support force of the beams predicted by ICFD with that of SPH. Table 2 shows a comparison of the maximum displacement and the peak force predicted by ICFD/SPH with the according experiments. The SPH method is predicting twice as much displacement as the ICFD method. This difference will be explained later in the paper.

Fig. 10 shows a snapshot of the water impacting the panel with the ICFD and SPH solutions. Notice the different effect and shape of the solid ICFD water and the SPH water particles.

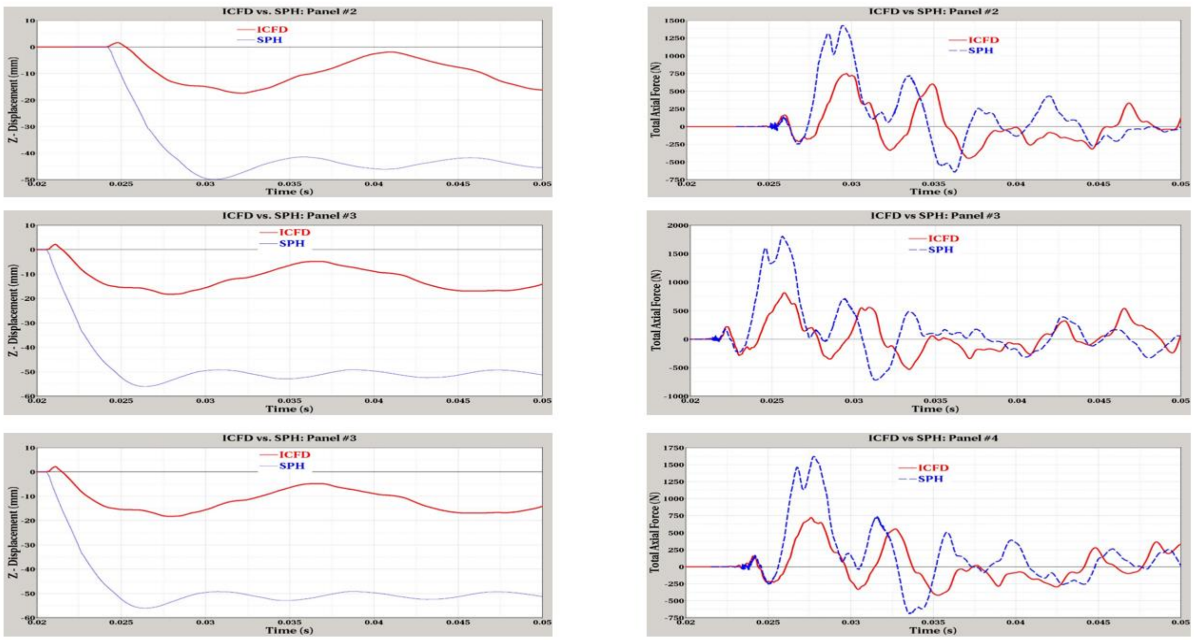

(a) ICFD (b) SPH

Fig. 9 Comparison of displacement and force profiles by ICFD and SPH (ICFD – red lines; SPH – blue lines).

Table 2 Comparison of maximum displacement and peak force by ICFD/SPH with experiment

Panel No.	Water Initial Velocity (m/s)	Peak Force (N)			Max. DIC Displ. (mm)		
		Exp.	ICFD	SPH	Exp.	ICFD	SPH
2	25.4	821.9	750.5 (-8.7%)	1428.4 (73.8%)	17.15	17.43 (1.6%)	49.93 (191%)
3	30.5	786.3	814.9 (3.65%)	1808.4 (130.0%)	17.74	18.29 (3.1%)	56.1 (216%)
4	27.9	1029	722.1 (-29.8%)	1625.2 (57.9%)	15.45	16.58 (7.3%)	53.1 (244%)

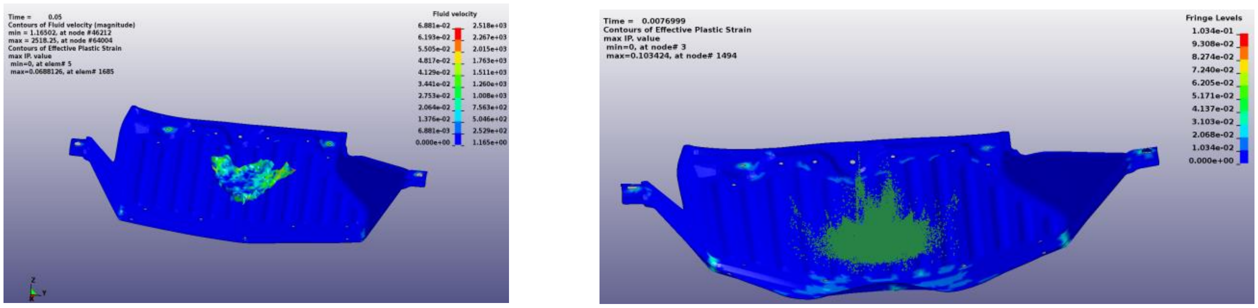

(a) ICFD (b) SPH

Fig. 10 Snapshot of the panel impacted by water body: (a) ICFD; (b) SPH

In this next section, it will be explained why SPH over predicts the results. Fig. 11 visually shows the reason. In the ICFD simulation, just before the water body contacts the panel, the shape of the water body is stretched and has a more slender cross-section. This results in a smaller impact area on the panel. It also shows that the velocity of the water has decreases slightly from the initial velocity. Developers at LSTC confirmed that the water geometry change is due to the adaptive meshing process in the ICFD solver. This caused an artificial friction effect applied on the water body while in motion. In contrast, in SPH method the water body holds its geometry and velocity before it reaches the panel which results in a comparatively larger impact area than in ICFD. Therefore, the SPH method produces a larger impact load on the panel.

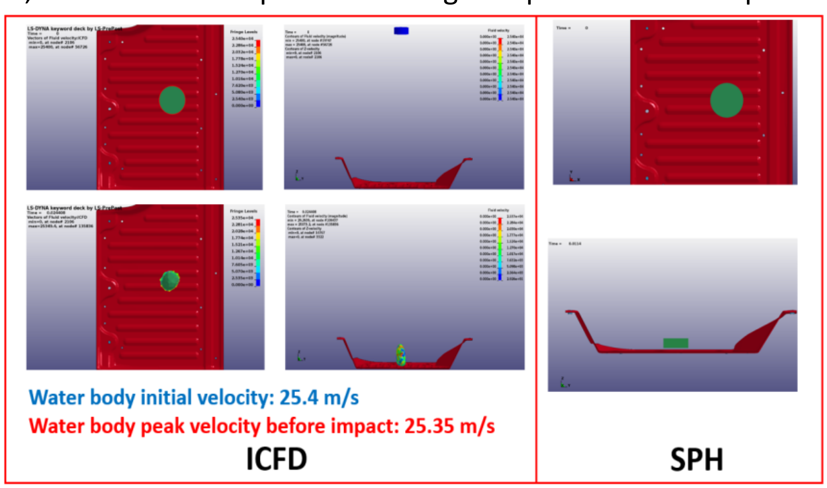

Fig. 11 Evolution of water body geometry and velocity in ICFD and SPH before contacting panel

A quick verification model was created and the results are shown in Fig. 12. This model shows that the dropping water ball holds its shape in the regular mesh zone but is stretched when entering the irregular mesh zone. This shape change in the ICFD solver matches the observations made in the high-speed test videos as seen in Fig. 13. A further verification can be made by adjusting the standoff distance in the model. Figure 14 shows the load and displacement results for a 24 in standoff (test condition) and 5.3 mm standoff (to hold initial water body shape before contact). It is clearly shown that the smaller standoff allows the water to retain its original shape which causes higher impact loads and displacements.

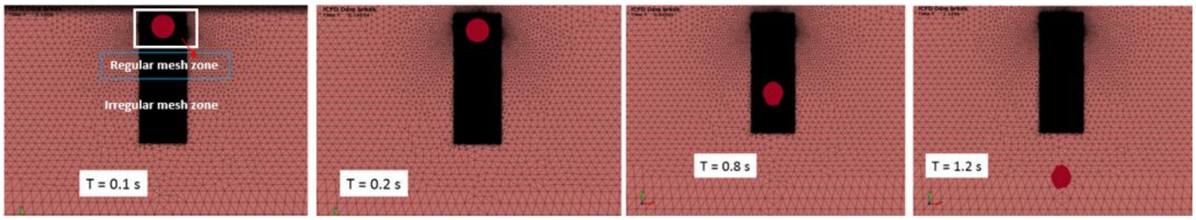

Fig. 12 Adaptive meshing effect on dropping water ball shape change in time.

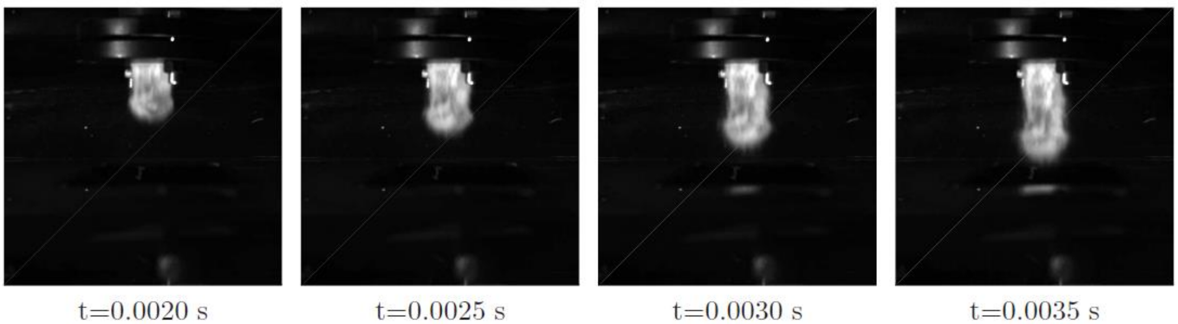

Fig. 13 Test data of water body geometry change before contacting panel.

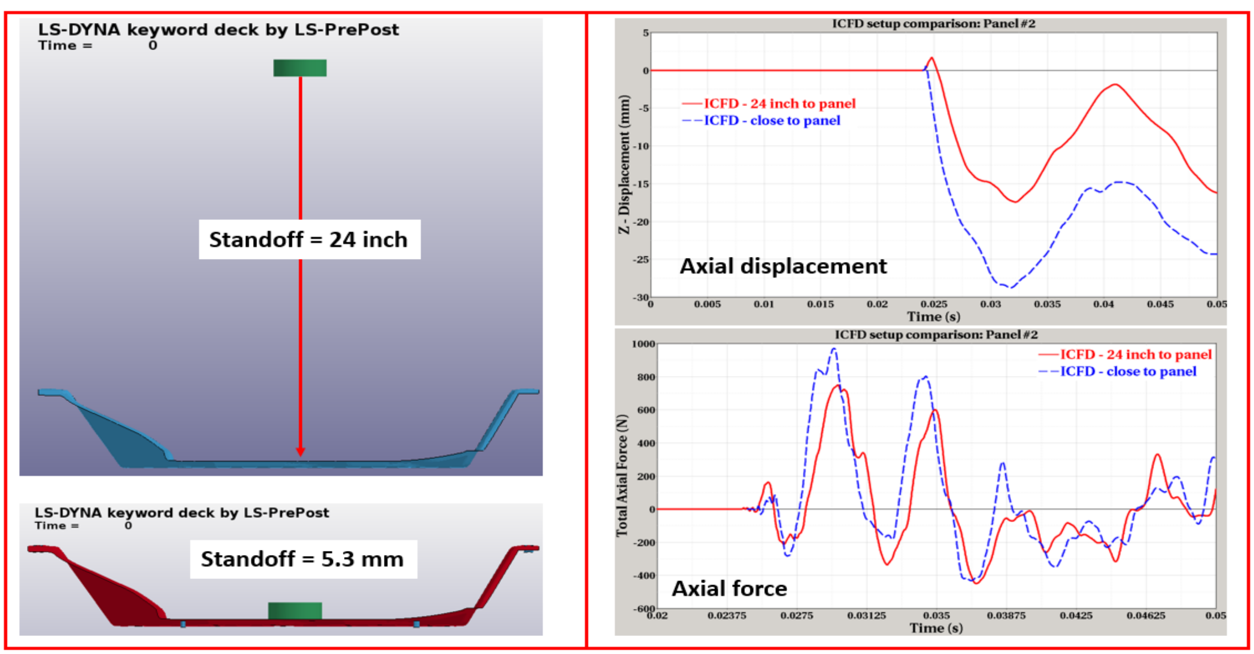

Fig. 14 ICFD standoff effect on impact results: 24 inch vs 5.3 mm

Table 3 shows the solution time of this model using the two methods. The SPH method is much more computationally efficient.

Table 3 Computation cost in ICFD and SPH

Panel No.	ICFD	SPH
2	1 hr. 42 min. 35 sec.	16 min. 29 sec.
3	2 hr. 56 min. 2 sec	15 min. 15 sec.
4	2 hr. 9 min. 50 sec	15 min. 58 sec.

2. Water splash impact on vehicle

In this study, a CAE model is developed to solve a half MUV running at 45 mph into a 0.24 m high water layer. ICFD and SPH are applied. The vehicle bottom surface is considered as a deformable structure while the other parts are rigid. The diameter for the tires is 0.67 m.

2.1 Model setup

Fig. 15 (a) shows the assembled ICFD fluid surface mesh. A fine mesh is applied to the water body (pid = 1) and the tires (pid = 3, 4) to capture the fluid-structure interaction while a coarse mesh is applied to the remaining parts. A non-slip condition is set to the flow boundary at the floor (pid = 2, 9) and solid parts (pid = 3,4,5). Air pressure is set to the lateral boundary (pid = 8). LES is selected for modeling the turbulent flow.

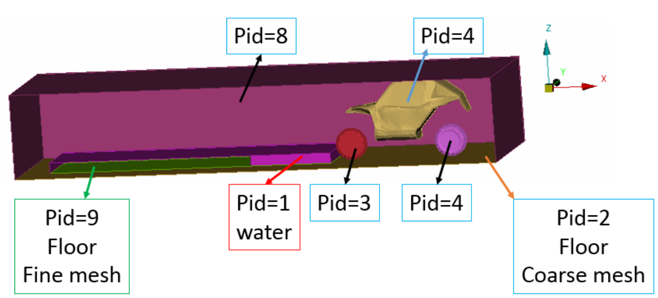

(a) ICFD fluid surface mesh

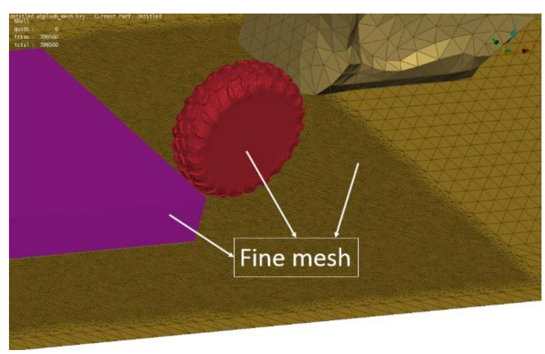

(b) solid structure mesh

Fig. 15 Assembled ICFD fluid surface mesh and solid mesh in a half MUV CAE model

Fig. 16 shows the solid structure mesh in the CAE model. The vehicle bottom material is steel (green part) and the remaining parts are rigid. The vehicle body parts are set with an initial translational speed of 45 mph and the two tires with the rotation speed matching the forward movement. The water body is approximated by 1,135,004 SPH particles with *MAT9.

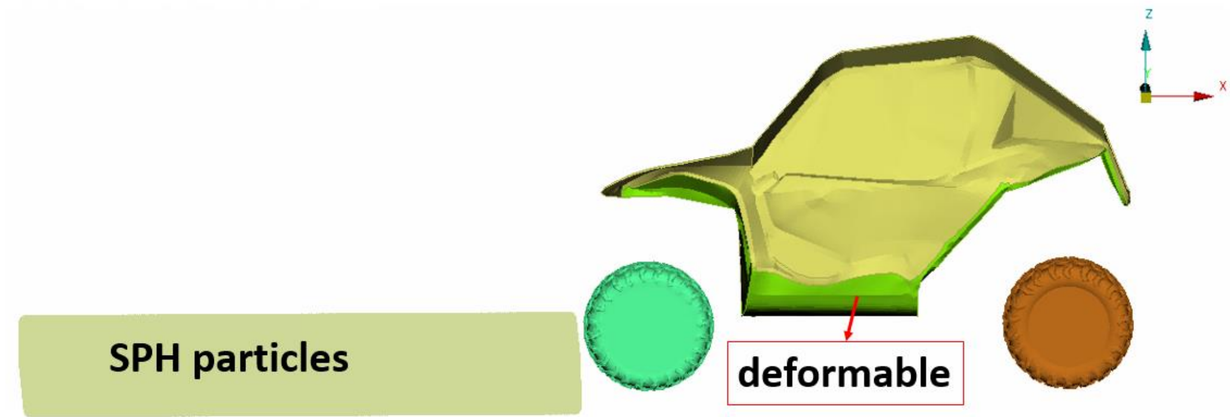

Fig. 16 Solid structure mesh of the MUV and the SPH mesh of the water

Fig. 17 (a-c) shows how the SPH method captures the detailed water splashing and interaction with the half MUV from different viewpoints.

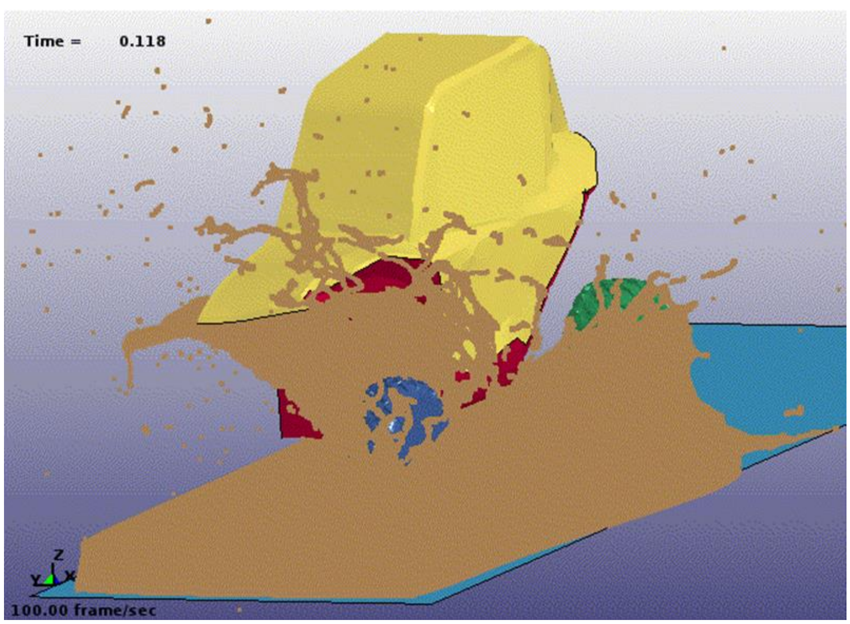

a) 3D view

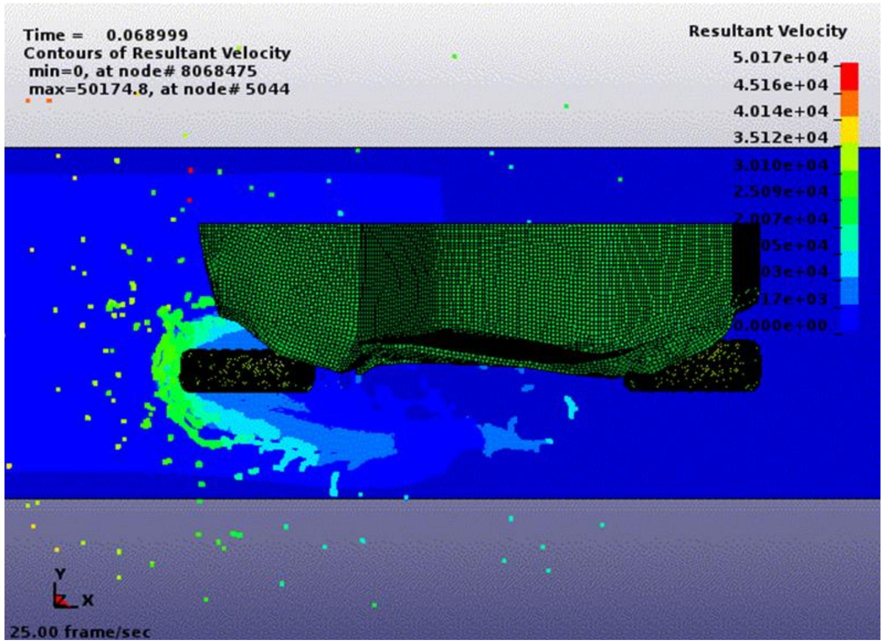

b) Top view

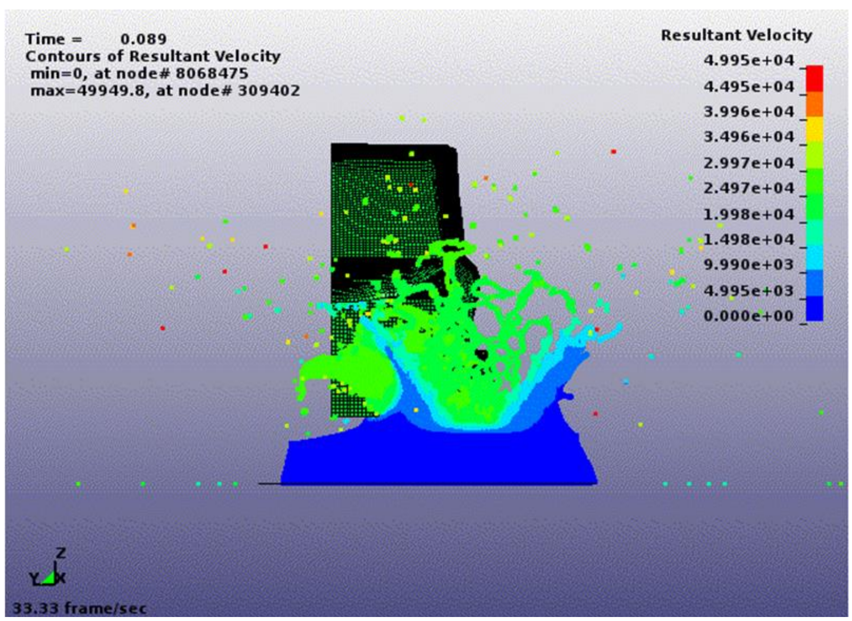

c) Front view

Fig. 17 SPH results of half MUV water splashing

Fig. 18 (a-c) shows the ICFD results of the half MUV water splashing seen from different viewpoints. The ICFD method has difficulty in predicting the detailed water splashing phenomena that was exhibited with the SPH method.

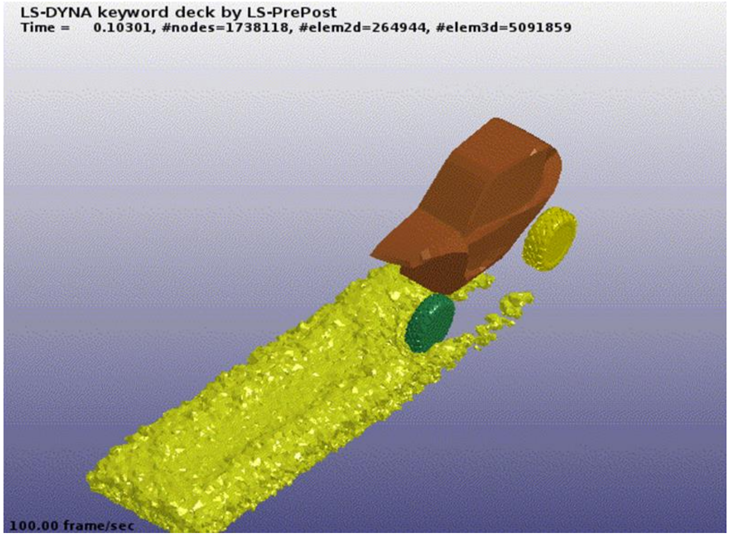

(a) 3D view

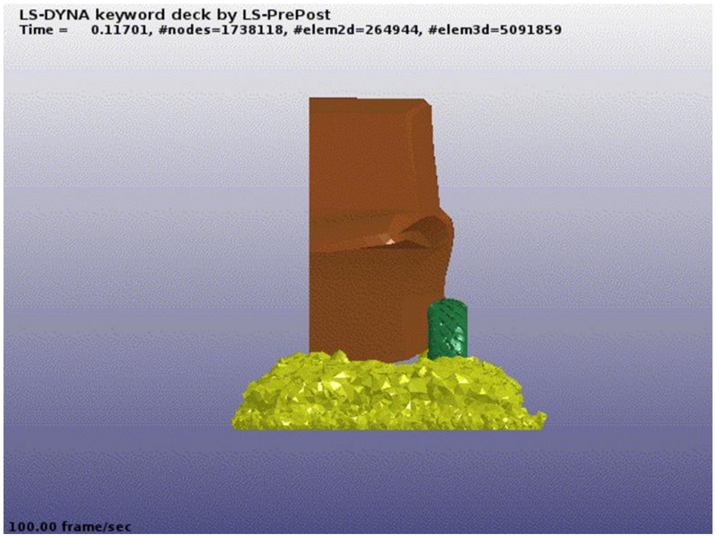

(b) Front view

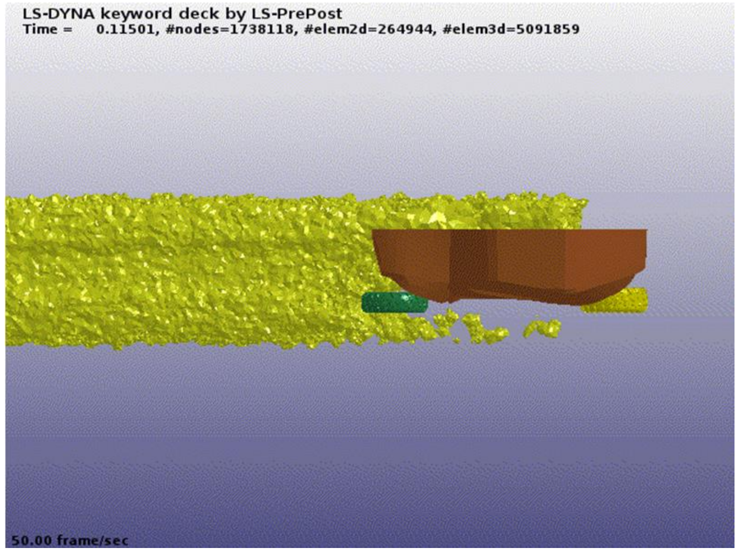

(c) Top view

Fig. 18 ICFD results of half MUV water splashing

Table 4 shows the solution time of this model using the two methods. The SPH method is much more computationally efficient.

Table 4 Computation cost by ICFD and SPH in a half-MUV FSI model

ICFD	SPH
73 hr. 57 min. 36 sec.	33 hr. 27 min. 23 sec.

Conclusions

Some FSI solutions of water splashing of automotive components by using ICFD and SPH solvers from LS-DYNA® were presented and good results are obtained:

(i) The aluminum panel is impacted by a water balloon shot out of a water cannon. Results with ICFD and SPH solvers are discussed and compared with the corresponding test data from the Ohio State University in Columbus, OH, USA. The ICFD results of displacement/force on the panel caused by the impact agree well with the tests while the SPH method over predicts the load/displacement.

(ii) A FSI model is developed to simulate a half MUV running at 45 mph into a 0.24 m high water layer. The vehicle bottom surface is set up as a deformable structure while the other parts are rigid. From the simulations it is found that the SPH method can easily simulate the realistic water splashing caused by the moving tires and vehicle body, whereas the ICFD solution has difficulty arriving at a solution and also takes much longer to solve.

Acknowledgements

This paper wishes to acknowledge the support from Glen Chamberlain in ISD at Honda R&D Americas, Inc.

References

1. *LS-DYNA® KEYWORD USER'S MANUAL VOLUME III Multi-Physics Solvers*, 10/21/16 (r:8003), LS-DYNA Dev, LIVERMORE SOFTWARE TECHNOLOGY CORPORATION (LSTC)
2. *LS-DYNA® Theory Manual*, 12/17/15 (r:7032), LS-DYNA Dev, LIVERMORE SOFTWARE TECHNOLOGY CORPORATION (LSTC)
3. Inaki Caldichoury, etc., *LS-DYNA®R7: Strong Fluid Structure Interaction (FSI) capabilities and associated meshing tools for the incompressible CFD solver (ICFD), applications and examples*, 9th European LS-DYNA Conference, Manchester, UK, 2013
4. Inaki Caldichoury, etc., *LS-DYNA®R7: Conjugate heat transfer problems and coupling between the incompressible CFD solver (ICFD) and the thermal solver, applications, results and examples*, 9th European LS-DYNA Conference, Manchester, UK, 2013
5. Inaki Caldichoury, etc., *LS-DYNA®R7: Coupled Multiphysics analysis involving Electromagnetism (EM), Incompressible CFD (ICFD) and solid mechanics thermal solver for conjugate heat transfer problem solving*, 9th European LS-DYNA Conference, Manchester, UK, 2013
6. Facundo Del Pin, etc., Advances on the Incompressible CFD Solver in *LS-DYNA®*, 11th International LS-DYNA® Users Conference, Detroit, USA, 2010
7. Bruno Boll, etc., *Coupled Simulation of the Fluid and Conjugate Heat Transfer in Press Hardening Process*, LS-DYNA Forum, Bamberg, 2014.
8. *LS-DYNA® KEYWORD USER'S MANUAL, VOLUME I*, 11/08/16 (r:8019), LS-DYNA Dev, LIVERMORE SOFTWARE TECHNOLOGY CORPORATION (LSTC)
9. R.A. Gingold and J.J. Monaghan, *Smoothed particle hydrodynamics: theory and application to non-spherical stars*, Mon. Not. R. Astron. Soc., Vol 181, pp. 375–89, 1977.
10. J. Xu and J. Wang, *Interaction Methods for SPH Parts (Multiphase Flows, Solid Bodies) in LS-DYNA®*, 13th International LS-DYNA Users Conference, Detroit, USA, 2016
11. J. Xu and J. Wang, *Node to node contact for SPH applied to multiple fluids with large density ratio*, 9th European LS-DYNA Users Conference, Manchester, UK, 2013
12. S. Tokura, *Comparison of Particle Methods: SPH and MPS*, 13th International LS-DYNA Users Conference, Detroit, USA, 2016